NASA TECHNICAL NOTE

NASA TN D-2122



NASA TN D-2122

# A MONTE CARLO CALCULATION OF THE NUCLEAR COLLISION DENSITY OF PRIMARY GALACTIC PROTONS IN A SLAB OF ALUMINUM

*by Millard L. Wohl*

*Lewis Research Center*
*Cleveland, Ohio*

NATIONAL AERONAUTICS AND SPACE ADMINISTRATION • WASHINGTON, D. C. • MARCH 1964

# A MONTE CARLO CALCULATION OF THE NUCLEAR COLLISION DENSITY OF PRIMARY GALACTIC PROTONS IN A SLAB OF ALUMINUM

By Millard L. Wohl

Lewis Research Center
Cleveland, Ohio

NATIONAL AERONAUTICS AND SPACE ADMINISTRATION

For sale by the Office of Technical Services, Department of Commerce,
Washington, D.C. 20230 -- Price $0.50

# A MONTE CARLO CALCULATION OF THE NUCLEAR COLLISION DENSITY OF PRIMARY GALACTIC PROTONS IN A SLAB OF ALUMINUM

by Millard L. Wohl

Lewis Research Center

## SUMMARY

A Monte Carlo code was written for the IBM 7090 computer. The code considers protons in the primary galactic energy range (0.1 to 10 Bev) impinging at angles of $0^{\circ}$, $30^{\circ}$, $45^{\circ}$, and $60^{\circ}$, as well as isotropically, on an infinite slab of aluminum 55 centimeters thick. The average proton nuclear collision density in each of six laminar regions of the slab is computed.

In addition, the energy distribution of evaporation neutrons from the resulting excited nuclei is computed, and the statistical model assumed to be valid. The proton collision density may be used as the spatial source density distribution for calculations of the transport of the secondary neutrons.

## INTRODUCTION

One of the crucial factors in the determination of the feasibility of extraterrestrial space flight is the provision of adequate shielding against the high-energy space radiation encountered. An important aspect of shielding studies directed to this end is consideration of secondary radiation produced in the shell of a space vehicle, which may be far more damaging to personnel or instrumentation than the much higher energy primary radiation responsible for its production.

Since estimates of the magnitudes of secondary-source intensities are needed, it was decided to compute, by the Monte Carlo method, the spatial and energy distribution of secondary evaporation neutron sources produced by high-energy primary galactic protons impinging at angles of $0^{\circ}$, $30^{\circ}$, $45^{\circ}$, and $60^{\circ}$, as well as isotropically, on a laterally infinite slab of aluminum 55 centimeters thick. Under the assumptions made, the spatial evaporation neutron source distribution is essentially equivalent to the proton nuclear collision density. In addition to energy degradation by nuclear collision, protons suffer ionization energy loss between nuclear collisions. The calculation does not include the intranuclear cascade process, which has been studied at length in the 0.025- to 0.4-billion-electron-volt energy range (ref. 1).

SYMBOLS

| | |
|---|---|
| $a$ | adjustable parameter |
| $E$ | emission energy of evaporation neutron, Mev |
| $F(\mu), G(\mu)$ | cumulative distribution functions for $\mu$ |
| $f(x)$ | probability density function for $x$ |
| $f(\mu), g(\mu)$ | probability density functions for $\mu$ |
| $g(y)$ | probability density function for $y$ |
| $g(E-x)$ | probability density function for $y$ |
| $h(E)$ | maxwellian probability density function for $E$ |
| $N$ | counting index |
| $N^*$ | computed evaporation neutron energy distribution |
| $P(\xi_M)$ | cumulative distribution function for $\xi_M$ |
| $p(s)$ | probability density function for proton intercollision path length |
| $p(\mu)$ | probability density function for $\mu$ |
| $p(\xi_M)$ | probability density function for $\xi_M$ |
| $s$ | nuclear intercollision distance |
| $s'$ | dummy variable of integration |
| $T$ | nuclear temperature, Mev |
| $x$ | dummy variable |
| $y$ | dummy variable, $E - x$ |
| $Z$ | coordinate axis designation |
| $z$ | normal distance from left side of slab |
| $\eta$ | frequency distribution for $E$ |
| $\theta_0$ | angle between incident proton direction and normal to slab boundary |
| $\lambda$ | proton mean free path for nuclear collision |
| $\mu$ | cosine of polar scattering angle |

$\xi_M$ maximum of finite set of pseudorandom numbers

$\xi_s$ specific pseudorandom number

$\xi_1, \xi_2, \xi_3, \xi_4$ pseudorandom numbers uniformly distributed in $0 \rightarrow 1$

$\xi'$ redefined pseudorandom number

$\Sigma_T$ total nuclear macroscopic cross section

$\sigma_i$ standard deviation of $\bar{\psi}_i$

$\psi$ azimuthal proton scattering angle

Subscripts:

i,j summation indexes

## ANALYSIS AND COMPUTING PROCEDURE

Throughout this discussion, frequent reference will be made to figure 1, which is the logical flow chart for the Monte Carlo computing process. The following discussion corresponds to the sequential logical portions of figure 1.

### Source Proton Energy Spectrum

The source spectrum used is a rough simplification of that given in reference 2 (a pointwise spectrum is assumed to hold over a continuous energy region) and is assumed to be of the form

$$\eta(E)dE \propto E^{-a}\, dE \tag{1}$$

where $a = 0.5$. A choice of source proton energy is made from this spectrum by a straightforward rejection technique, as illustrated by branch A of figure 1.

### Source Proton Direction

The geometric configuration and the incident-proton direction are illustrated in the following sketch:

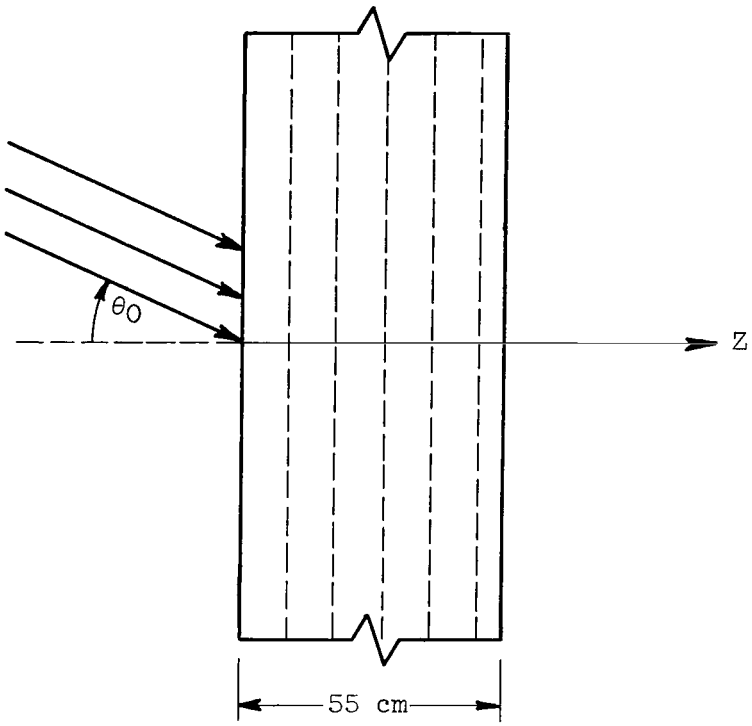


The angle $\theta_0$ may have a value of $0^\circ$, $30^\circ$, $45^\circ$, or $60^\circ$.

## Distance to Nuclear Collision

The distance to a nuclear collision is selected, as is customary, from the following exponential distribution:

$$p(s)ds = \Sigma_T e^{-\Sigma_T s}\, ds \tag{2}$$

where $p(s)$ is the probability of collision in $ds$ about $s$. Mapping equation (2) onto a space of the $0 \rightarrow 1$ uniform random variable $\xi$ gives

$$\left.\begin{aligned} \Sigma_T \int_0^s e^{-\Sigma_T s'}\, ds' &= \xi \\ s = -\frac{1}{\Sigma_T} \ln \xi &= -\lambda \ln \xi \end{aligned}\right\} \tag{3}$$

The values of $\xi$ are generated by a double-entry subroutine that uses the method of congruences (ref. 3). The proton mean free path for nuclear collision used is 42 centimeters over the energy range considered (0.1 to 10 Bev). This is an average of three values given in reference 4. The z-coordinate of the nuclear

collision point is compared with the slab thickness of 55 centimeters. If either $z > 55$ centimeters or $z < 0$, the history counter is incremented by one and a new history begun. If $0 \leq z \leq 55$ centimeters, the appropriate one of six z-bin counters designated by ANS(KKK) in figure 1 is incremented by one. (Symbols used in fig. 1 are defined in the appendix.)

## Energy Loss Between Nuclear Collisions

Between nuclear collisions, the proton suffers a continuous ionization energy loss due to electromagnetic interaction with electron and ion fields. The energy loss in the intercollision transit is established by finding the energy corresponding to the residual range of the proton, the difference between the range (which refers only to ionization slowing down) and the nuclear intercollision distance. The maximum of the latter, of course, is the full range. The range-energy data for protons in aluminum given in reference 5 are used herein. Branches C and D of figure 1 describe the computation of the energy EE after ionization slowing down.

## Description and Kinematics of Nuclear Collision

When the proton nuclear collision kinematics were considered, it was decided to idealize the process as follows:

(1) The proton suffers a knock-on direct nonrelativistic collision with a loosely bound nucleon; thus hydrogen-like scattering kinematics may be used.

(2) A sufficient number of nuclear energy levels are excited so that the statistical, or "temperature," model of nuclear excitation is valid (ref. 6).

(3) Only evaporation neutron emission is considered.

The collision mechanics are as follows: The probability density function for the cosine of the proton polar scattering angle is, as is the case with neutron-hydrogen collisions,

$$p(\mu) = 2\mu \tag{4}$$

In order to sample from this distribution, consider the following (ref. 7):

(1) Let $\mu$ = largest $(\xi_1, \xi_2, \ldots, \xi_N)$, where the $\xi$'s are pseudorandom numbers.

(2) If $\xi_M$ is the largest of $(N - 1)$ $\xi$'s, the cumulative distribution function for $\xi_M$ is

$$P(\xi_M) = \xi_M \xi_M, \ldots, \xi_M = \xi_M^{N-1}$$

since the probability that a pseudorandom number is less than or equal to $\xi_M$ is merely equal to $\xi_M$. The corresponding probability density function is thus

$$p(\xi_M) = \xi_M^{N-2}(N - 1) \tag{5}$$

(3) Consider another $\xi = \xi_s$ and let $\mu$ = larger $(\xi_M, \xi_s)$.

(4) Then

$$\begin{aligned} p(\mu) &= f(\mu)G(\mu) + F(\mu)g(\mu) \\ &= (N - 1)\mu^{N-2}\mu + \mu^{N-1} \\ &= N\mu^{N-1} \end{aligned} \tag{6}$$

where $f$ and $g$ are probability density functions, and $F$ and $G$ are cumulative distribution functions. Since $N = 2$ (eq. (4)), a sample may be obtained from the distribution $p(\mu) = 2\mu$ by setting

$$\mu = \text{larger } (\xi_1, \xi_2) \tag{7}$$

After a value of $\mu$ has been determined, a new z-direction cosine is computed by means of the cosine law for spherical triangles, as in branch E of figure 1. The azimuthal scattering angle $\psi$ is chosen uniformly between 0 and $2\pi$ by means of the von Neumann rejection technique (ref. 8), also described in branch E of figure 1.

It is assumed that each nuclear proton collision gives rise to nuclear excitation and the subsequent production of an evaporation neutron from an ensemble whose energy distribution is given by

$$h(E) \propto Ee^{-E/T}$$

where $T$, the nuclear temperature parameter, was chosen to be 12 million electron volts.[1] In order to sample from the distribution

$$h(E) \propto Ee^{-E/T} \tag{8}$$

set

$$E = -T \ln(\xi_1\xi_2) \tag{9}$$

In order to prove this, let

$$E = -T \ln(\xi_1\xi_2) = -T(\ln \xi_1 + \ln \xi_2) \tag{10}$$

If

[1]This value was suggested by R. M. Sternheimer in a private communication.

$$\left.\begin{aligned} x &= -T \ln \xi_1 \\ \text{and} \\ y &= -T \ln \xi_2 \end{aligned}\right\} \qquad (11)$$

it is known that

$$\left.\begin{aligned} f(x) &= \frac{1}{T} e^{-x/T} \\ \text{and} \\ g(y) &= \frac{1}{T} e^{-y/T} \end{aligned}\right\} \qquad (12)$$

where $f$ and $g$ are the probability density functions of $x$ and $y$, respectively.

Now, the joint probability density function is

$$h(E) = \int_0^E f(x)g(E - x)dx$$

$$= \frac{1}{T^2} \int_0^E e^{-x/T} e^{-(E-x)/T} dx \qquad (13)$$

$$= \frac{1}{T^2} E e^{-E/T} \qquad (14)$$

Thus, the sampling prescription described by equation (9) produces the correct probability density function $h(E)$ (eq. (14)).

Since information on relative evaporation neutron yields is unavailable at this time in the 0.4- to 10-billion-electron-volt proton energy range, an evaporation neutron is assumed generated and an energy picked every time a proton nuclear collision occurs. A histographic energy distribution is thus accumulated during the calculation. This is indicated in branch F of figure 1.

If the transport of secondary neutrons were of interest, the proton collision density would provide the spatial source distribution, the energy distribution would be given by figure 2, computed from equation (9), and the angular distribution could be assumed isotropic.

## History Termination

Each time a proton is slowed down, either by ionization or collision, its

energy is compared with the cutoff energy, 0.101 billion electron volt. If the energy is above the cutoff point, the history is continued. If the energy is below the cutoff point, the history is terminated. A history is also terminated if $z < 0$ or $z > 55$ centimeters, as mentioned previously.

## Statistical Analysis

Since the integral of the collision density in a given z-bin is tabulated by a pure counting procedure, the statistical variation of this quantity may be described by a Poisson distribution. Thus, the fractional standard deviation of $\bar{\psi}_i$, the mean collision density in the $i^{th}$ bin, is given by (ref. 9)

$$\frac{\sigma_i}{\bar{\psi}_i} = \frac{\left[\int_{z_i}^{z_{i+1}} \bar{\psi}_i(z)\,dz\right]^{1/2}}{\bar{\psi}_i(z_{i+1} - z_i)} \qquad (i = 1, 2, \ldots, 6) \tag{15}$$

In branch G of figure 1, a calculation of fractional standard deviations of the $\bar{\psi}_i$'s is carried out on the basis of an examination of the spread of results of 50 subgroups, each containing averages of 100 histories. The counterpart of equation (15) is

$$\frac{\sigma_i}{\bar{\psi}_i} = \left[\frac{\sum_{j=1}^{50} (\bar{\psi}_i - \psi_{ij})^2}{49}\right]^{1/2} \qquad (i = 1, 2, \ldots, 6) \tag{16}$$

## DISCUSSION OF RESULTS

The computed proton nuclear collision densities for incidence angles of $0^\circ$, $30^\circ$, $45^\circ$, and $60^\circ$, as well as isotropic incidence, are displayed in figure 3. Since the slab thickness considered is 55 centimeters, or only 1.25 proton mean free paths, it is to be expected that the angle of incidence will play an important role in determining the collision density. This is indeed the case and is clearly demonstrated by the increase of collision density with incidence angle in the shallow portions of the slab, as shown in figure 3.

In most of the cases considered, the fractional standard deviation of the collision density, according to equation (15), is a few percent. The fractional standard deviations computed from equation (16) are about 25 percent, which demonstrates the relative inaccuracy of the method of equation (16) for the subgroup size (100 histories) and the total number of histories run (5000).

The computed secondary neutron energy distribution (fig. 2) displays the maxwellian shape prescribed by equation (14). The most probable energy is about 12 million electron volts, which is to be expected, in view of the temperature

of nuclear excitation assumed. A secondary neutron spatial source distribution equivalent to the proton nuclear collision density may be assumed for the investigation of secondary neutron transport.

Lewis Research Center
National Aeronautics and Space Administration
Cleveland, Ohio, October 10, 1963

## APPENDIX - FLOW-CHART SYMBOLS

| Branch | Symbols | Definition |
|---|---|---|
| AA | NCHIS | number of case histories |
| | cos $\theta$ | z-direction cosine, $\Omega_z$ |
| | EE | proton energy prior to nuclear collision, Bev |
| A | F(EE) | source energy distribution function |
| | K | normalization constant for source energy distribution |
| | AMAX | maximum value of source energy distribution |
| | RAT | ratio of F(EE) to AMAX |
| B | $\lambda$ | proton mean free path |
| | Z | z-coordinate of collision point |
| | ZB | proton nuclear intercollision distance |
| C | E(K),R(K) | discrete energies and corresponding proton ranges in aluminum; E(K) in Bev, R(K) in cm |
| | RR | proton range |
| | ZP | residual proton range |
| D | KKK | proton collision counter index |
| E | $\psi$ | azimuthal scattering angle |
| | $\mu$ | cosine of polar scattering angle |
| | $\omega$ | polar scattering angle |
| | ANS(KKK) | contents of each of six proton collision counters |
| F | ENERGY(NN) | contents of secondary neutron energy bin |
| G | NFIN | total final number of proton histories (5000 in this calculation) |
| | GRPFIN(I) | average of collision density over 5000 histories |

| Branch | Symbols | Definition |
|---|---|---|
| | GRPAVG(I,NUMINT) | average of collision density over 100 histories |
| | SUM(I) | fractional standard deviation of collision density with 100-history subgroups |

## REFERENCES


1. Bertini, H. W.: Monte Carlo Calculations on Intranuclear Cascades. ORNL-3383, AEC, May 1963.

2. Condon, E. U., and Odishaw, Hugh, eds.: Handbook of Physics. McGraw-Hill Book Co., Inc., 1958, pp. 9-208.

3. Taussky, O., and Todd, J.: Symposium on Monte Carlo Methods. John Wiley & Sons, Inc., 1956, p. 17.

4. More, K., Tiffany, O. L., and Wainio, K.: Cosmic Ray Shower Production in Manned Space Vehicles. Paper presented at Conf. on Medical and Biological Problems in Space Flight (Nassau), Nov. 1961.

5. Sternheimer, R. M.: Ionization and Range Curves Including Corrections for Density. Techniques of High Energy Phys., David M. Ritson, ed., Intersci. Pub., Inc., 1961, pp. 526-531.

6. Goldstein, Herbert: Fundamental Aspects of Reactor Shielding. Addison-Wesley Pub. Co., Inc., 1959.

7. Kahn, Herman: Applications of Monte Carlo. RM-1237, AEC, 1956.

8. Meyer, Herbert A., ed.: Symposium on Monte Carlo Methods. John Wiley & Sons, Inc., 1956, p. 93.

9. Beers, Yardley: Introduction to the Theory of Error. Addison-Wesley Pub. Co., Inc., 1953, p. 45.

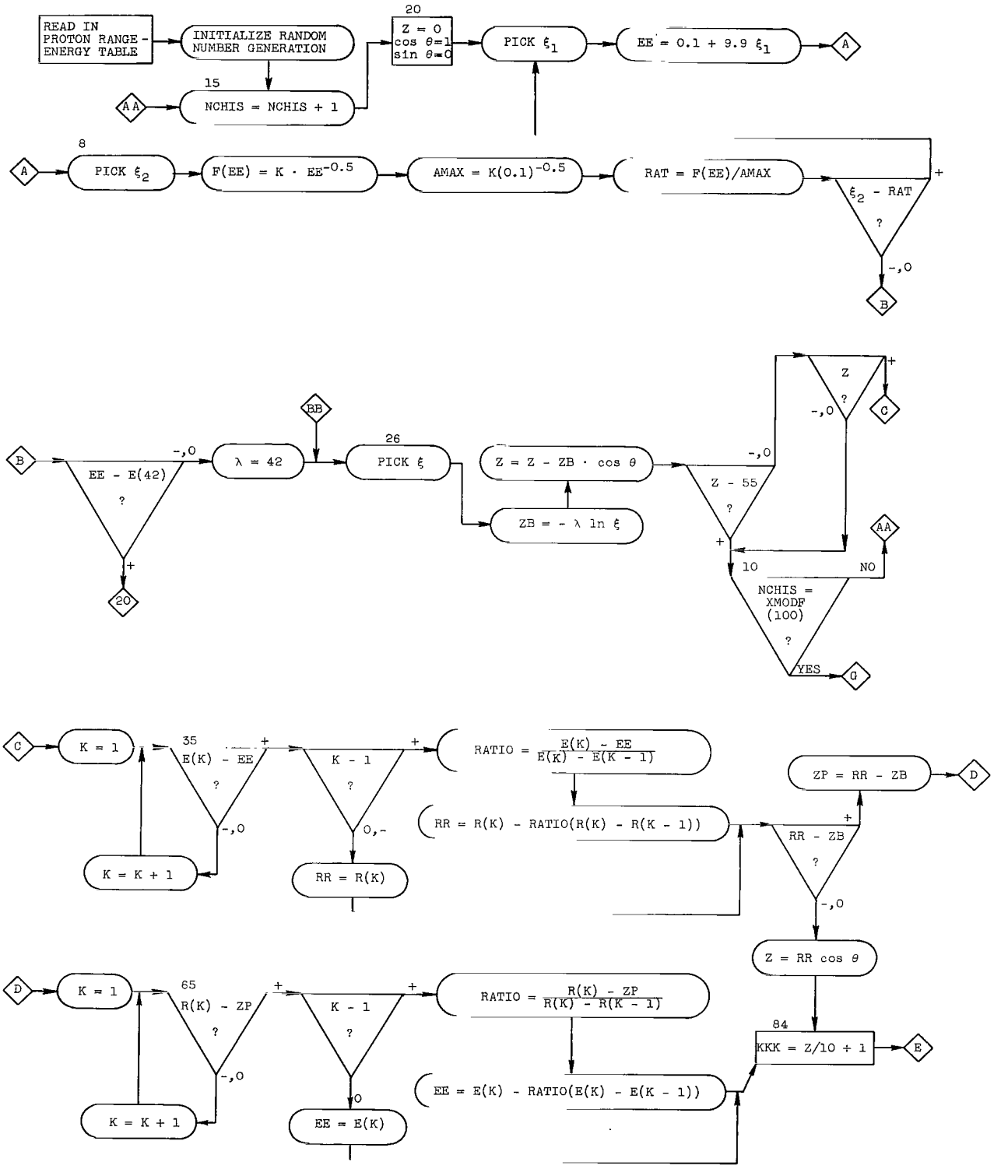


(a) Branches A to D.

Figure 1. - Monte Carlo flow chart.

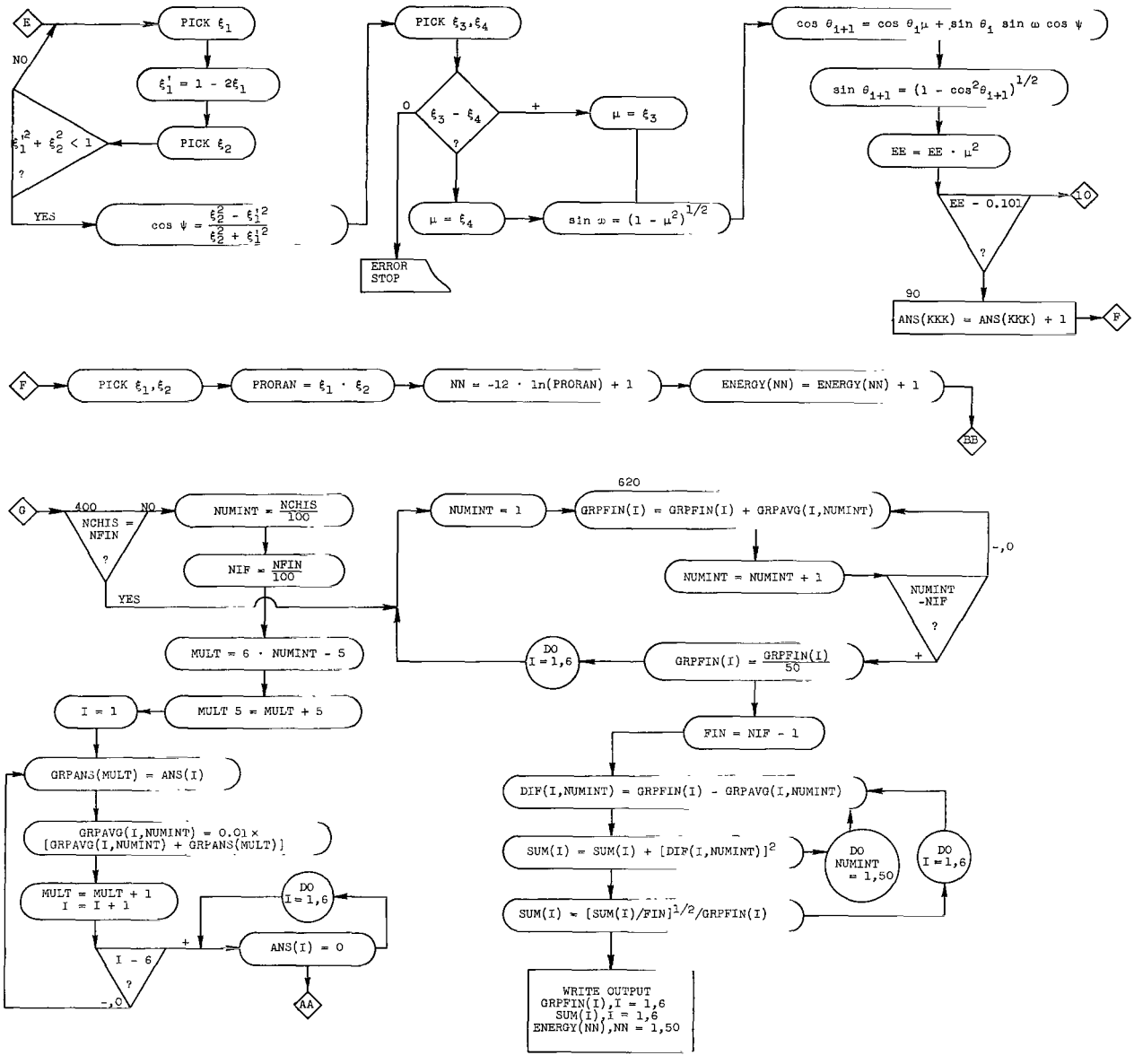


(b) Branches E to G.

Figure 1. - Concluded. Monte Carlo flow chart.

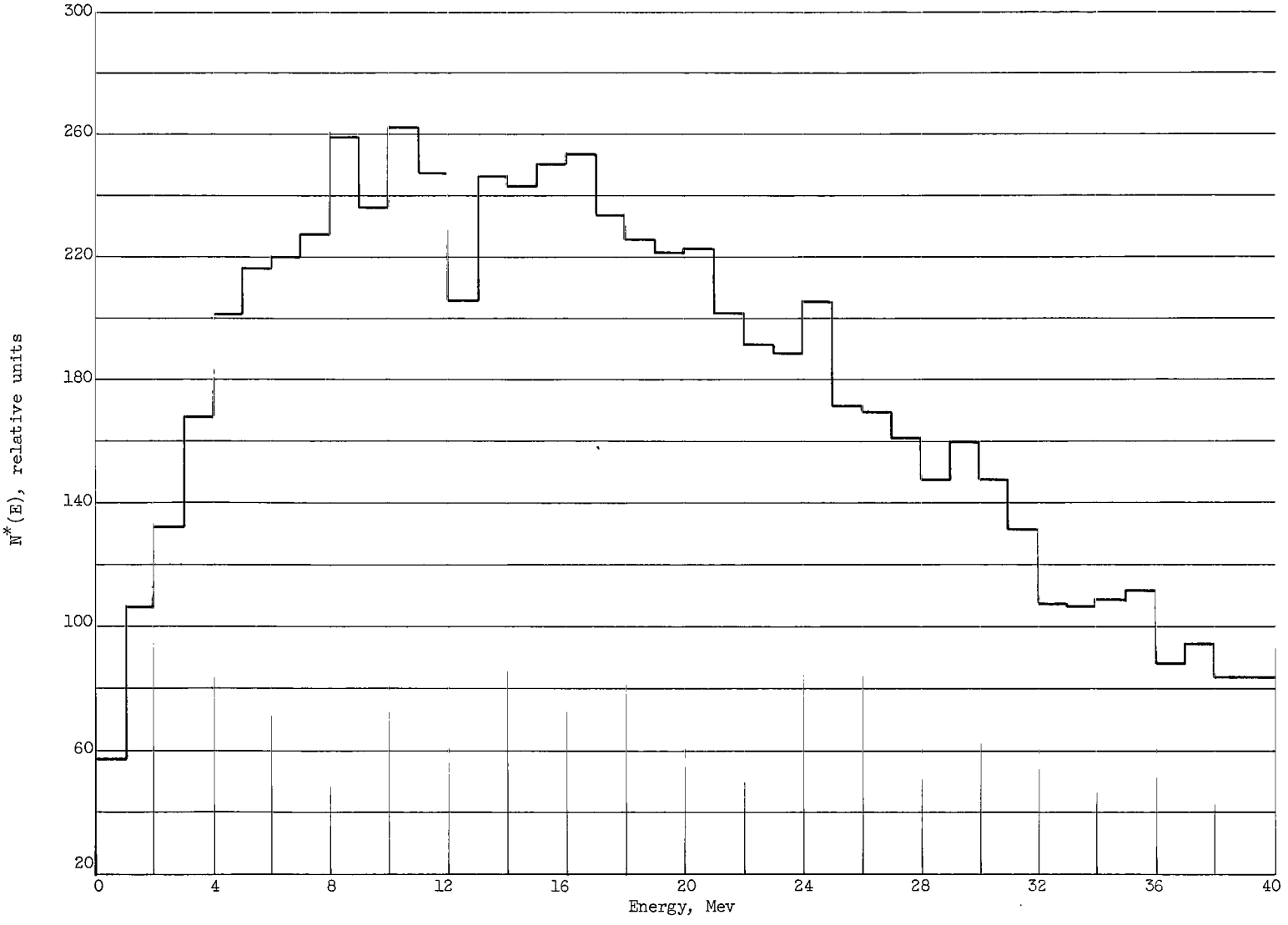


Figure 2. - Energy distribution of evaporation neutrons.

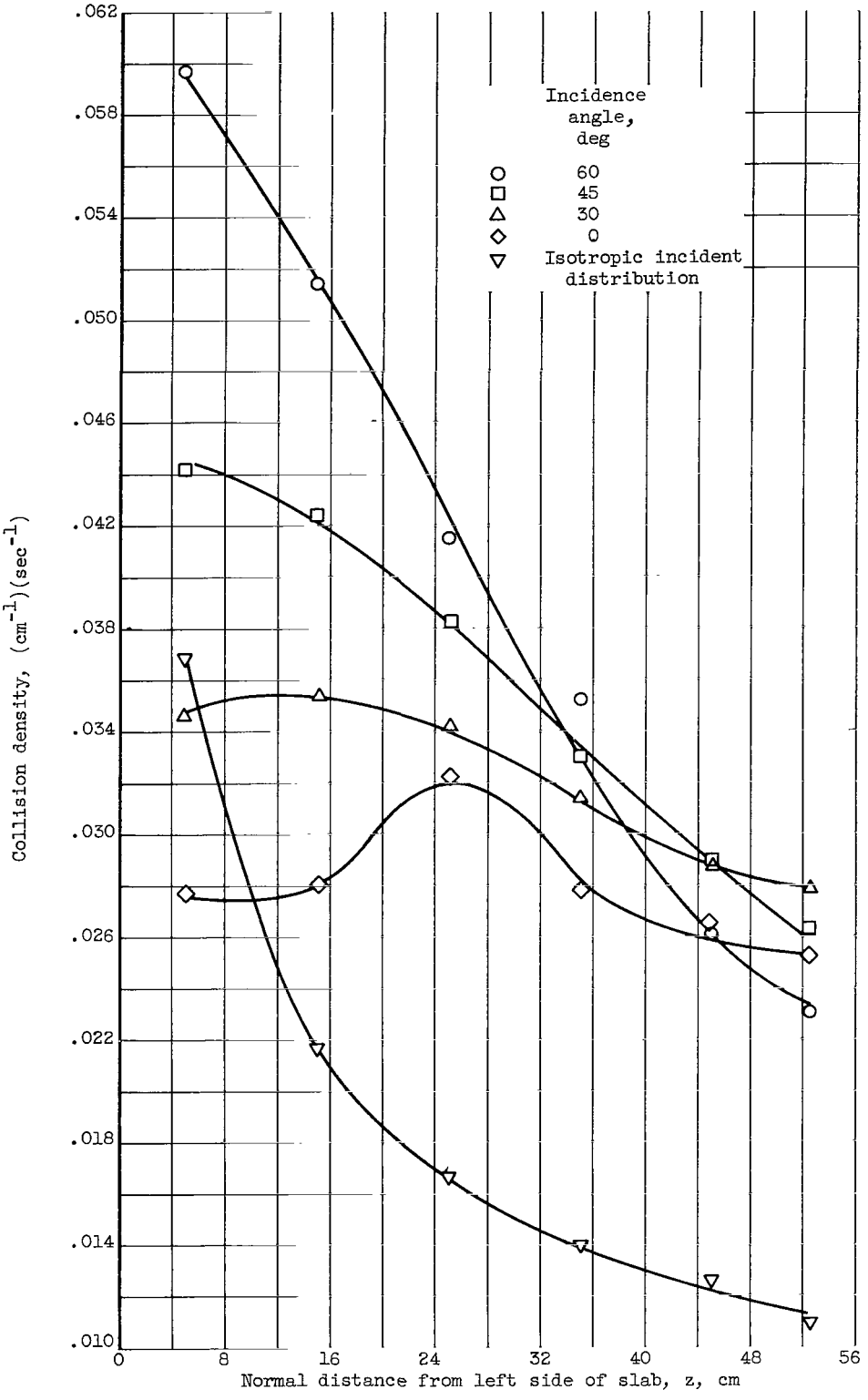


Figure 3. - Proton nuclear collision density as function of penetration depth in slab. (Source normalized to 1 proton per second.)